

CHAPTER THIRTEEN

Deformation, Metamorphism, and Time

13.1	Introduction	316	13.6	<i>D-P-T-t</i> Paths	329
13.2	Field Observations and Study Goals	316	13.6.1	Temperature-Time (<i>T-t</i>) History	331
13.3	Pressure and Temperature	319	13.6.2	Pressure-Temperature (<i>P-T</i>) History	331
	13.3.1 Status Report I	321	13.6.3	Pressure-Time (<i>P-t</i>) History	331
13.4	Deformation and Metamorphism	322	13.6.4	The Geothermal Gradient	331
	13.4.1 Status Report II	324	13.6.5	The Deformational Setting	333
13.5	Time	325	13.7	Closing Remarks	333
	13.5.1 The Isochron Equation	325		Additional Reading	333
	13.5.2 The Isotopic Closure Temperature	327			
	13.5.3 Dating Deformation	328			
	13.5.4 Status Report III	329			

13.1 INTRODUCTION

Unraveling the deformation history of a region is somewhat like a “whodunit” mystery. Well, it perhaps isn’t quite as exciting as some of the stuff in the movies, but a mystery it is. Just like any modern detective you need tools in the forensics lab to solve the geologic mystery. While it is impossible to be expert in all of today’s methods (ranging from materials science to chemistry), a basic knowledge is required to help you decide what may be useful for your particular case. In this essay we look at some approaches, mainly from the fields of metamorphic petrology and isotope geochemistry, that are integral parts of many studies of deformed regions. We concentrate on medium- to high-grade metamorphic areas, which are representative of processes that are active in the deeper levels of the crust, to complement the emphasis on shallow-level deformation earlier in the book. We use a hypothetical area with hypothetical (i.e., perfect?) rocks,¹ in

¹While based on real geographic names and natural rocks, any resemblance to reality is purely coincidental.

order to show the complementary nature of other approaches to “traditional” structural analysis. As we go along, you will find that this chapter remains far from comprehensive; hence we call it an essay.

First we need to collect, organize, and examine the evidence, and then chart our course of action. Some of the associated terminology and concepts that will follow are listed in Table 13.1 for reference.

13.2 FIELD OBSERVATIONS AND STUDY GOALS

We are studying the tectonic evolution of a metamorphic terrane containing rocks in greenschist to granulite facies. Our first field summer was used to map the lithologies and structure of the area. Now that we have a basic understanding of the structural geometry (i.e., locations of shear zones, nature of fabrics, and so on), we select samples for laboratory analysis (Figure 13.1a). The goal of our study is to determine the spatial and temporal conditions at which these rocks were deformed. Specifically, we try to determine the crustal

TABLE 13.1 SOME TERMS AND CONCEPTS RELATED TO DEFORMATION, METAMORPHISM, AND TIME

(Geo)barometry	Determination of pressure during metamorphism.
(Geo)chronology	Isotopic age determination of a mineral or rock; these ages are given in years. Sometimes called “absolute” age.
Clockwise <i>P-T-t</i> path	Burial history plotted in <i>P-T</i> space of rapidly increasing temperature relative to pressure followed by uplift history of rapidly decreasing pressure relative to temperature. <i>Note:</i> Clockwise is defined in a <i>P-T</i> plot with <i>P</i> increasing downward; petrologists use the opposite terminology because they plot <i>P</i> increasing upward.
Closure temperature	Temperature at which a system becomes closed to loss of the radiogenic daughter isotope.
Cooling [rate]	Temperature decrease [with time].
Counterclockwise <i>P-T-t</i> path	Burial history plotted in <i>P-T</i> of rapidly increasing pressure relative to temperature followed by uplift history of rapidly decreasing temperature relative to pressure. Counterclockwise is defined with <i>P</i> increasing downward.
Exhumation [rate]	Displacement relative to the surface [with time]; also <i>denudation</i> , <i>unroofing</i> .
Geothermal gradient	Temperature change per depth unit [typically °C/km or K/km].
<i>P-T-t</i> path	History of rock or region in pressure(<i>P</i>)-temperature(<i>T</i>)-time(<i>t</i>) space.
Paragenesis	Mineral assemblage in a metamorphic rock.
Peak metamorphism	Condition of peak-temperature and corresponding pressure. Note that peak temperature generally does <i>not</i> coincide with peak pressure [and vice versa].
Porphyroblastesis	Relative timing of mineral growth with respect to deformation (strictly: mineral growth).
Postkinematic growth	Metamorphic mineral growth after deformation.
Prekinematic growth	Metamorphic mineral growth before deformation.
Prograde metamorphism	Metamorphic history before peak-temperature, characterized by dehydration reactions and density increase.
Retrograde metamorphism	Metamorphic history after peak-temperature condition, which may involve hydration reactions in the presence of an H ₂ O-rich fluid.
Synkinematic growth	Metamorphic mineral growth during deformation.
Tectonite	General term for a deformed rock; the adjectives L, S, and L-S indicate dominance of a lamination, a foliation, or a combination, respectively.
(Geo)thermobarometry	Temperature–pressure determination using equilibrium reactions.
(Geo)thermochronology	Temperature–time history of rocks.
(Geo)thermometry	Determination of metamorphic temperature.
Uplift [rate]	Displacement relative to a fixed reference frame, such as the geoid [with time].
(Mineral) zonation	Presence of compositionally distinct regions in a mineral grain; this records changing conditions of chemical equilibrium during growth or subsequent modification at times of chemical disequilibrium. Typically zonation is found from core to rim in such minerals as garnet and feldspar.

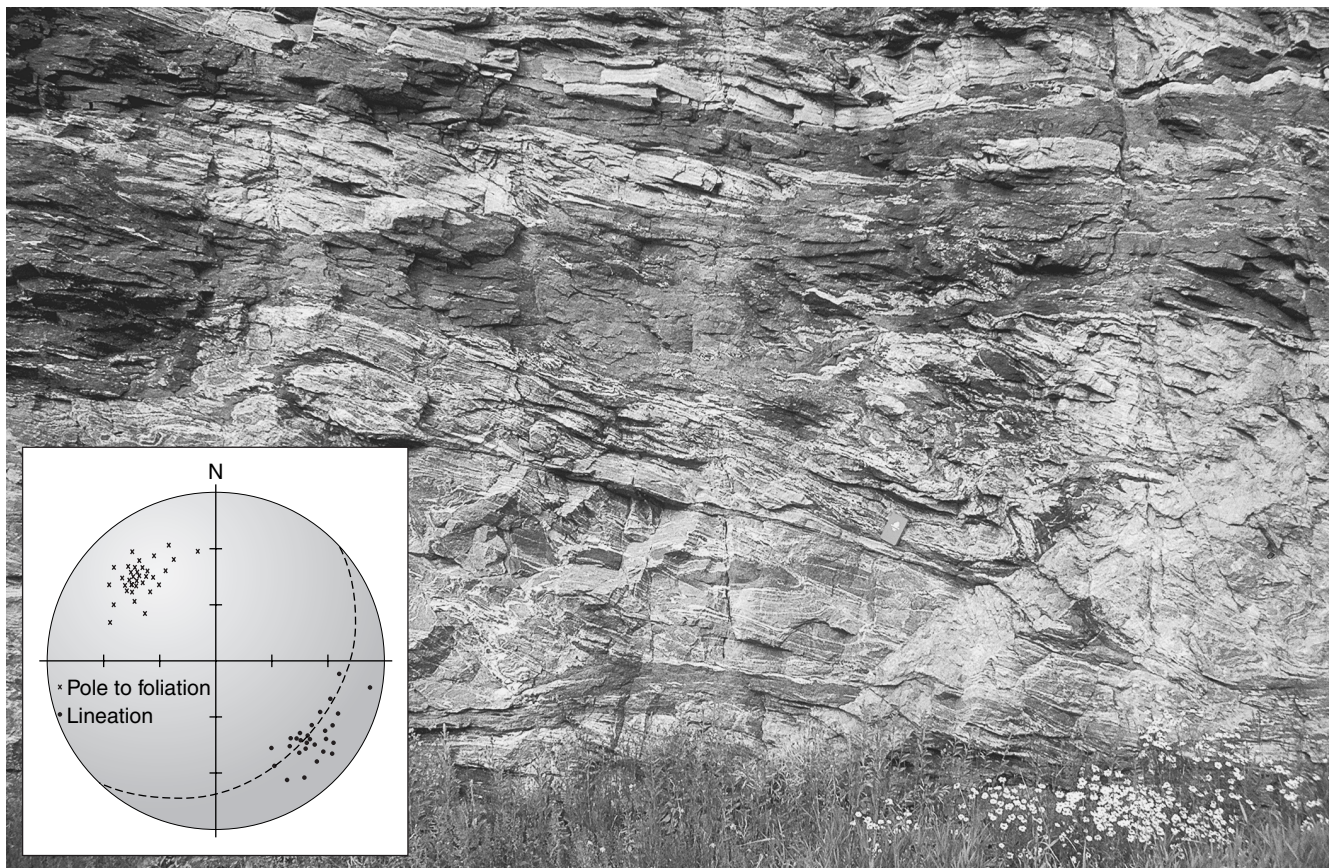


FIGURE 13.1 Field photograph of mylonitic gneiss used in our analysis and corresponding lower hemisphere, equal-area projection of spatial data (inset).

depth at which these rocks were deformed, the timing of metamorphic and deformational events, and their burial and exhumation history in the context of tectonic evolution.

Our rocks are called *paragneiss* and *marble*, which are metamorphic rocks of sedimentary origin (as opposed to *orthogneiss*, which is a metamorphic rock of igneous origin). Prior to removing samples, we characterize the outcrop as a whole and carefully orient our specimens by marking dip and strike or dip direction on the samples. These **tectonites** have several field characteristics. Most obvious is a well-developed foliation that is defined by compositional variation or color banding, and a lineation that is defined by oriented hornblendes in the paragneiss and black graphitic stripes in the marble. The orientation of these fabric elements in outcrop is shallowly SE-dipping and SE-plunging, respectively. Upon detailed inspection of the gneiss, we see a fine matrix that surrounds millimeter-size grains with distinct shapes and textures. In particular, the asymmetry of tails on feldspar grains in the gneiss draws our attention, because it indicates a left-lateral sense of displacement along the foliation when looking to the northeast

(δ -type clasts; Section 12.3.2). Based on the presence of a strongly foliated and lineated fabric, fine grain size of the rocks relative to neighboring outcrops, and the occurrence of shear-sense indicators, we conclude that the rock is a mylonite; that is, the rock was subjected to significant shear strain and deformed by crystal-plastic processes. We plot the spatial information in spherical projection (Figure 13.1 inset) and, based on the collective information, we conclude that the outcrop is part of a low-angle, SE-dipping shear zone with a reverse sense of displacement.

The paragneiss contains the minerals hornblende, garnet, quartz, feldspar, biotite, muscovite, and kyanite, and accessory phases that cannot be conclusively identified with the hand lens. This mineral assemblage suggests that the rock was metamorphosed in the amphibolite facies, indicating a temperature range of 500°C to 700°C and a pressure range of 400–1200 MPa (Figure 13.2). Staining of the marble with a solution of HCl and red dye indicates the presence of dolomite in addition to calcite; the main accessory phase is graphite. The assemblage of minerals in the marble does not allow us to determine the metamorphic grade in the field, but the coexistence of calcite and dolomite will be useful in the

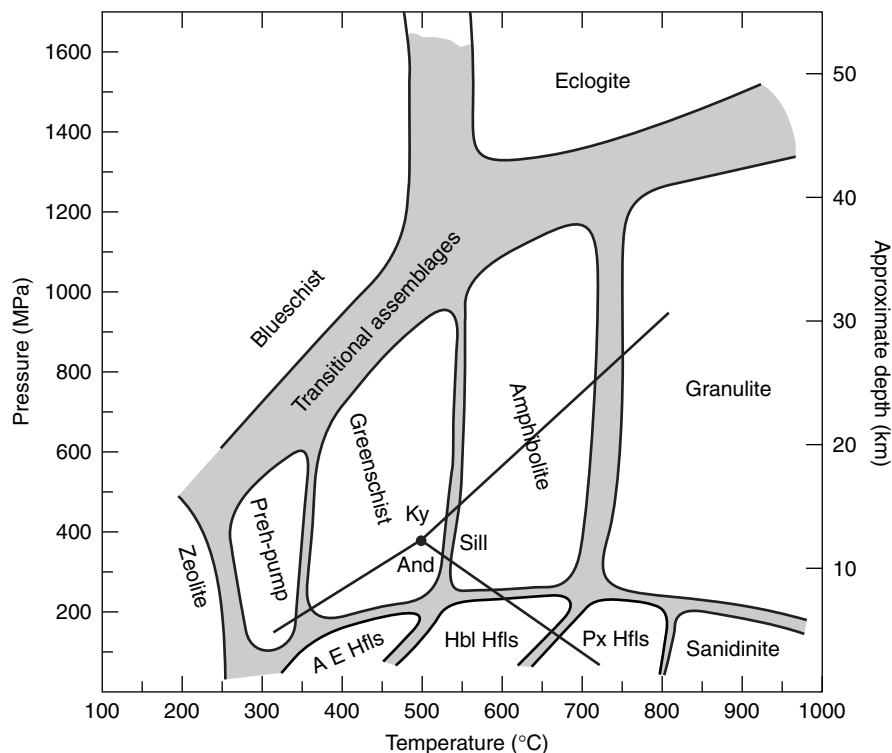


FIGURE 13.2 Pressure-temperature diagram showing the fields of the various metamorphic facies and the kyanite[Ky]-andalusite[And]-sillimanite[Sill] triple point. The approximate crustal depths that correspond to lithostatic pressures are also shown. Abbreviations used are: A-E = albite-epidote, Hbl = hornblende, Hfils = hornfels, Preh-Pump = prehnite-pumpellyite, Px = pyroxene.

laboratory as a geothermometer. After taking some photographs of the scene and making some sketches of geometric relationships, the samples are removed from the outcrop, labeled, and taken to the laboratory for further analysis.

Upon returning to the bug-free environment of the laboratory, we cut oriented samples and prepare two mutually perpendicular thin sections. The sections are oriented such that one is perpendicular to foliation and parallel to lineation, and the other is perpendicular to both foliation and lineation. These two surfaces provide a three-dimensional description of the microscopic characteristics of each sample. Thin sections of the gneiss reveal that our field conclusions about metamorphic grade were generally correct. The main minerals in the rock are plagioclase and alkali feldspar, quartz, hornblende, biotite, muscovite, garnet, and kyanite, and the accessory phases are rutile, ilmenite, and titanite (also called sphene). The foliation is defined by alternating light and dark bands, whose color is a consequence of the relative proportion of light-colored quartz and feldspar, and dark-colored hornblende and biotite in these layers. The marble consists of calcite, dolomite, and minor amounts of graphite, monazite, and titanite. The foliation in the marble is defined by alternating layers of different grain size and by concentrations of opaques (mainly graphite) and other accessory phases.

13.3 PRESSURE AND TEMPERATURE

We first constrain the metamorphic conditions of our samples. **Geothermobarometry** is the quantification of temperature (T) and pressure (P) conditions to which a rock was subjected during its metamorphic history. It contributes three very important pieces to our geologic puzzle: (1) the peak temperature condition, (2) the approximate depth to which the rocks were buried (from pressure determination), and (3) (part of) the prograde and retrograde history of the rock. We will look at each piece in turn.

Experimental and thermodynamic work in metamorphic petrology, supported by empirical observations, have identified a large number of mineral reactions that can be used to estimate the P and T conditions of metamorphism. In making such estimates, it is assumed that the mineral assemblage or parts of individual minerals represent *equilibrium conditions*, which means that at a given condition of pressure and temperature certain minerals have specific compositions. Mineral assemblages make good geobarometers if the equilibrium reaction is relatively insensitive to temperature (Figure 13.3). Similarly, a good geothermometer is largely pressure independent (Figure 13.3); thermodynamically, this means there is

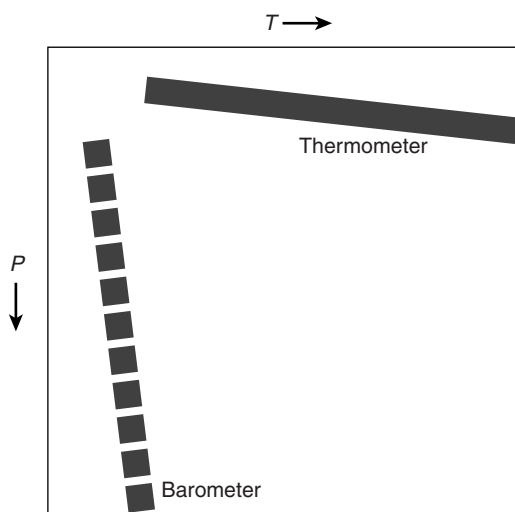


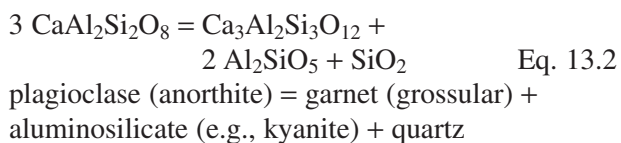
FIGURE 13.3 Reliable geothermometers (solid band) are largely pressure insensitive, whereas good geobarometers (dashed band) are largely temperature independent; they are schematically plotted in P - T space.

a large entropy² change, but little volume change in geothermometers. For example, consider the following reaction involving the exchange of ions:



where A and B are two minerals in equilibrium (e.g., garnet and biotite) and i and j are two cations (e.g., Fe^{2+} and Mg). Because only cation exchange occurs in this reaction, there is little or no change in volume involved, and consequently these types of reactions are pressure insensitive.

Now let's look at a geobarometer. The mineral garnet is common in amphibolite facies rocks, and is formed when the rocks contain sufficient amounts of the respective elemental constituents of that mineral. An example of a common garnet-forming reaction in metasediments is



Garnet is formed by the breakdown of plagioclase with increasing pressure. This particular reaction (also

²Entropy, S , is the thermodynamic parameter describing the degree of randomness (or disorder) in a system.

TABLE 13.2	SELECTED GEOBAROMETERS AND GEOTHERMOMETERS
<i>Geobarometers:</i>	
Garnet-plagioclase [reactions involving Ca exchange between garnet and plagioclase, for example, garnet-plagioclase-quartz- Al_2SiO_5 (GASP); garnet-plagioclase-rutile-ilmenite-quartz (GRIPS); garnet-rutile-ilmenite- Al_2SiO_5 -quartz (GRAIL)]	
Pyroxene-plagioclase-quartz (Na or Ca exchange)	
Phengite (phengite content in muscovite)	
Hornblende (Al content)	
<i>Geothermometers:</i>	
Garnet-biotite (Fe-Mg exchange)	
Garnet-pyroxene (Fe-Mg exchange)	
Two-feldspar (Na exchange between alkali feldspar and plagioclase)	
Two-pyroxene (Ca-Mg exchange)	
Calcite-dolomite (Mg exchange)	
Calcite-graphite (^{13}C isotopic fractionation)	
In part after Essene (1989).	

known by the acronym GASP³) is a geobarometer because it involves significant volume change, but is relatively insensitive to temperature. Thus, in a plot of pressure versus temperature (Figure 13.3), we find that lines with a shallow slope are good barometers and those with steep slopes are good geothermometers. Intermediate slopes indicate sensitivity to both pressure and temperature (one reaction, two unknowns), so the reaction can be used only if one parameter is determined independently.

A single mineral reaction describes a line in the P - T diagram; for example the kyanite-sillimanite boundary in Figure 13.2. Two mineral reactions define a single point in a P - T diagram, provided that the lines intersect; the greater the angle between the two intersecting lines the more reliable the P - T estimate. Examples of some widely used geothermometers and geobarometers are listed in Table 13.2; for details of these systems

³(G)arnet + (A)luminosilicate + (S)ilica = (P)lagioclase (silica is quartz).

and their applications you are referred to an extensive petrologic literature (see “Additional Reading”).

In theory, the application of thermobarometric systems should give unique, internally consistent values for pressure and for temperature, but in practice this is rarely the case. Nevertheless, with multiple reactions you are generally able to constrain the pressure conditions within ± 100 MPa (i.e., ± 1 kbar) and temperature conditions within $\pm 50^\circ\text{C}$. In all our future results we assume these practical error estimates.

After considering the mineral assemblage in our samples, we decide to apply the GASP and GRIPS geobarometers, and two-feldspar and garnet-biotite geothermometers to the paragneiss. Recall that the most reliable results are obtained when more than one system is used to determine P or T . The marble from the same outcrop does not contain an assemblage that allows pressure determination, but the calcite-dolomite and calcite-graphite systems are good geothermometers. After many hours in a darkened microprobe room and some stable isotopic work using a mass spectrometer (neither of which we describe here), we obtain an internally consistent pressure of 700 MPa (7 kbar) and a temperature of 600°C for our samples. These results place the rocks firmly in the amphibolite facies, just above the kyanite-sillimanite boundary (Figure 13.2).

What do these values of temperature (T) and pressure (P) really mean? In theory, thermobarometry measures the conditions at the time of mineral formation or when chemical exchange between phases ceases to occur. If the mineral formed during **prograde metamorphism** (i.e., there is a history of increasing metamorphic temperature), we assume that the temperature represents the peak temperature of metamorphism, because at these conditions the rate of mineral growth is highest. However, the chemical composition of minerals formed at peak temperature conditions may be modified during cooling of the rock, which is called **retrograde metamorphism**. Retrograde metamorphism may be preserved in zoned minerals, where only part of the mineral reequilibrates, or it may lead to complete compositional resetting. The latter is like erasing with one hand what you write on a board with the other. The rock achieves equilibrium for certain temperature conditions until this thermally activated process is too slow to allow further exchange.

The pressures that we derive from geobarometry do not describe the stress state that caused deformation of the rock. This is an important point. Rather, metamorphic pressures are lithostatic pressures and measure the weight of the overlying rock column (recall

Chapter 3). So, if we know the density of the rock column, we can translate metamorphic pressures into values for depth. For every kilometer of depth in the average crust the pressure increases by about 27 MPa (assuming an average rock density of 2700 kg/m^3 ; Chapter 3). Thus, the previously determinate pressure estimate of 700 MPa for our sample implies that these rocks were buried to a depth of about 26 km.

Zoned minerals are particularly useful for deciphering P - T history, because zonation records changes in conditions during prograde and/or retrograde metamorphism. Often the rims of minerals reset during retrograde P - T conditions. Zonation is sometimes visible in the optical microscope, but is usually determined using an electron microprobe, which recognizes small compositional differences. Mineral zonation stems from the incomplete equilibration of previously formed minerals. Garnets, which are particularly prone to zonation, are relatively fast-growing minerals that act as a memory of the metamorphic history. Figure 13.4 shows an example of a large garnet that preserves a complex history of growth, based on the irregular Ca pattern, and retrograde exchange, established from the decreasing Mg/Fe ratio (Mg decreases and Fe increases) and increasing Mn content toward the rim. From our garnet sample we are able to determine pressure and temperature for both core and rim of the mineral. The analysis of garnet cores and inclusions were given earlier (700 MPa, 600°C) and we obtain rim values of 500 MPa and 550°C .

13.3.1 Status Report I

What have we learned so far? After the gneiss and marble were deposited at the surface (they are metasediments!), they were buried by about 25 km where they became exposed to a peak temperature of 600°C (“core” P - T). Today these rocks are back at the surface, because we were able to sample them, and indeed they preserve a record of lower temperatures and pressures, during their ascent, as the “rim” P - T data (550°C at ~ 19 km depth). There is no record of shallower conditions because the kinetics (or rate) of the geothermobarometric reactions was too low. Thus, we are beginning to unravel a detailed burial and exhumation history, or the **P - T - t path**, of our rocks, which we eventually integrate with the structural evolution of our area. But before we can do this, we need to establish absolute and relative temporal relationships of deformation and metamorphism.

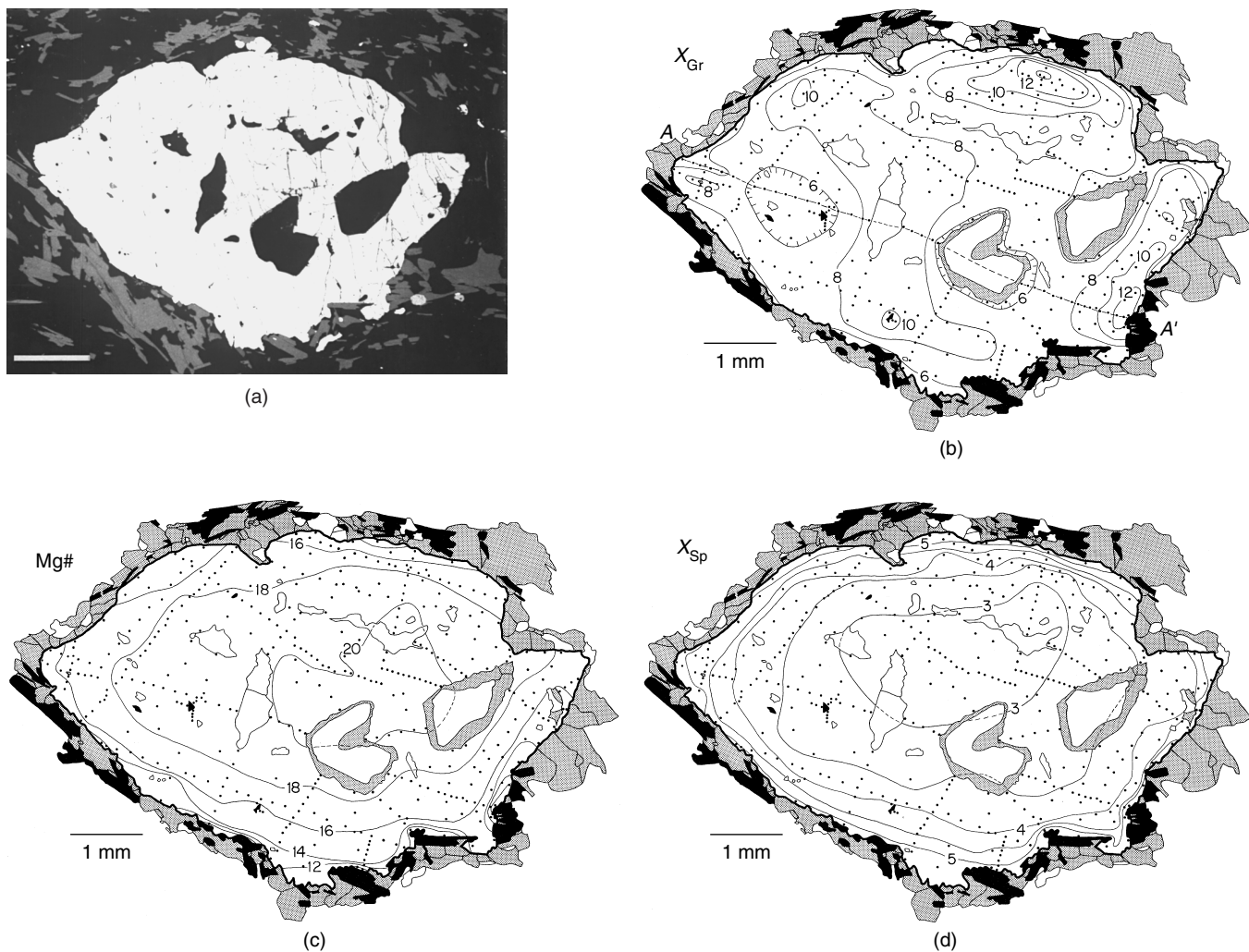


FIGURE 13.4 Complexly zoned, inclusion-rich garnet from the Grenville Orogen, showing (a) back-scattered electron image, and (b) Ca [$X_{Gr} = 100 \times \text{Ca}/(\text{Ca} + \text{Mn} + \text{Mg} + \text{Fe})$], (c) Mg# [$= 100 \times \text{Mg}/(\text{Mg} + \text{Fe})$], and (d) Mn [$X_{Sp} = 100 \times \text{Mn}/(\text{Ca} + \text{Mn} + \text{Fe})$] composition based on detailed electron microprobe analysis. Each dot in garnet represents an analytical point; black is biotite, gray is plagioclase, and white is quartz. Scale bar is 1 mm; zonation is given in mol%.

13.4 DEFORMATION AND METAMORPHISM

To understand the conditions during deformation, we must determine the relative timing of metamorphism with respect to deformation. **Prekinematic growth** means that mineral growth occurs before deformation, **synkinematic growth** means that growth occurs during deformation, and **postkinematic growth**, you guessed it, implies that minerals grow after deformation. The shape and internal geometry of minerals and their relationship to external fabric elements, in particular foliations, help us to determine this relative temporal relationship. Such newly grown minerals are

called **porphyroblasts**, derived from the Greek word “blastos” for growth, and the relationship between growth and deformation is called **porphyroblastesis**.

The beautiful crystals that decorate geodes may come to mind when thinking of mineral growth, but rocks at depths beyond a few kilometers rarely have any open spaces. Mineral growth under these conditions mostly occurs by the replacement of preexisting phases. For example, garnet grows by the consumption of another mineral, and phases that are not involved in the reaction (accessory phases such as zircon, monazite), or phases that are left over because the rock does not contain the right mix of ingredients, may become inclusions. These inclusions may form

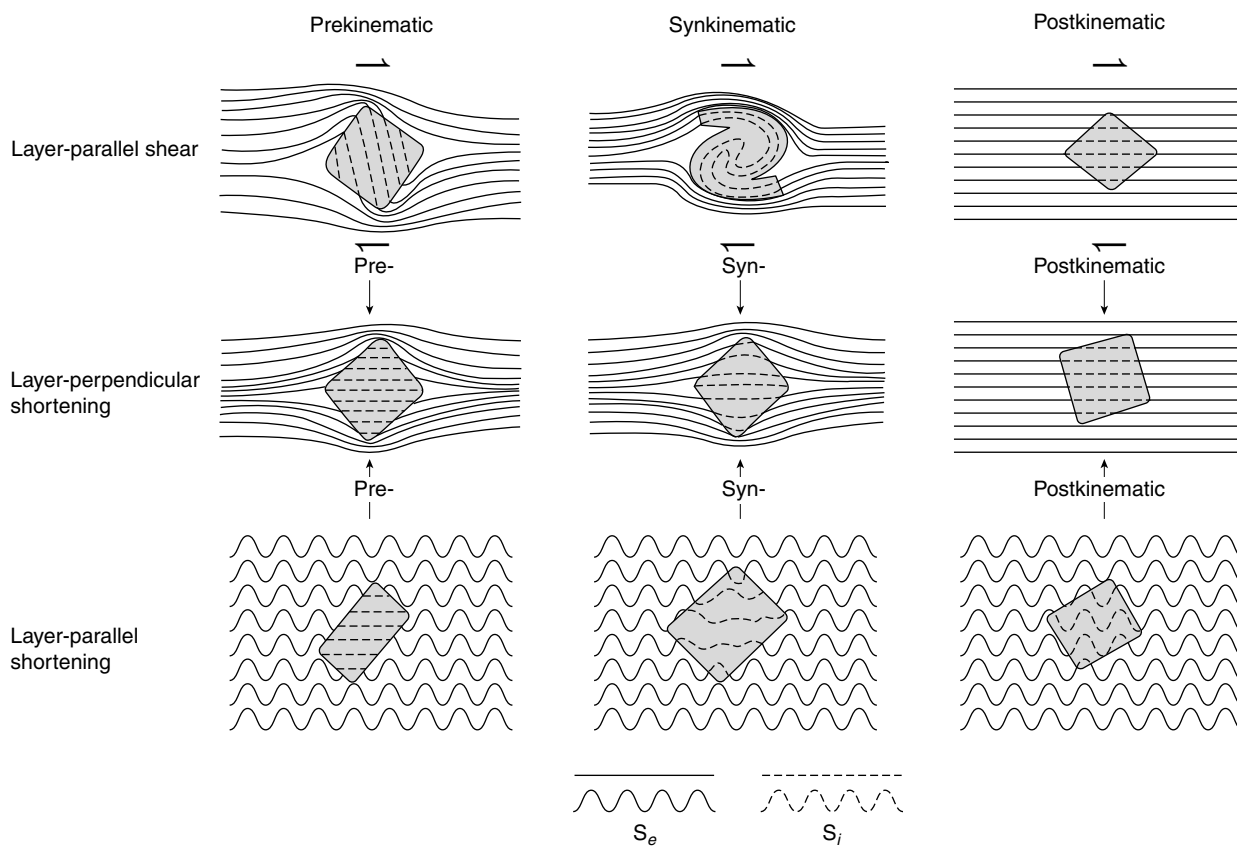
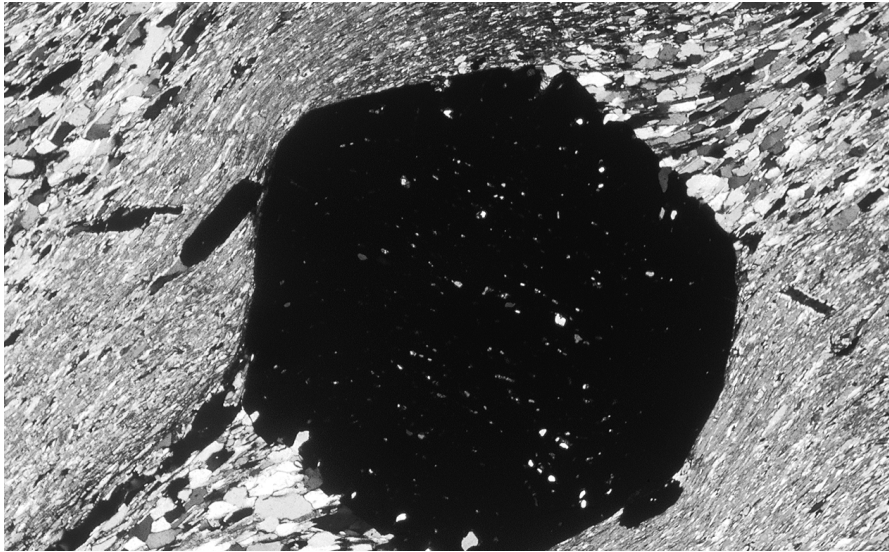


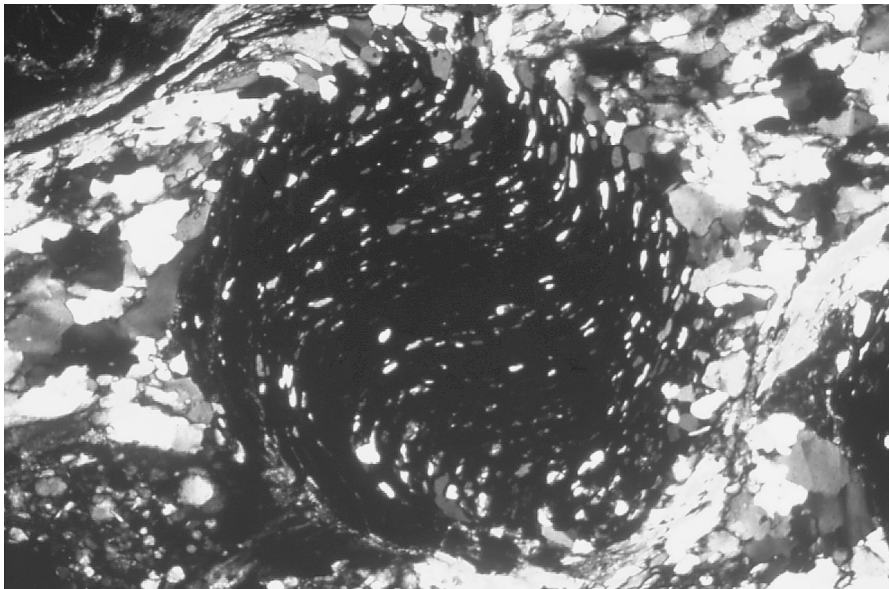
FIGURE 13.5 Schematic diagram showing the diagnostic forms of porphyroblasts that grow before [prekinematic], during [synkinematic], and after [postkinematic] layer-parallel shear, layer-perpendicular shortening, and layer-parallel shortening. The temporal relationship is based largely on the relationship between the internal foliation (S_i ; dashed lines) and the external foliation (S_e ; solid lines).

ordered trails that define an **internal foliation** (S_i) in the porphyroblast; for contrast, the foliation outside the blast is called the **external foliation** (S_e). The relationship between S_i and S_e allows us to determine the relative timing of mineral growth and deformation (Figure 13.5). Prekinematic growth is characterized by an internal foliation (S_i) whose shape is unrelated to S_e , and typically the internal and external foliations do not connect. At the other end of the spectrum we find postkinematic growth, which shows an external foliation that continues into the grain seemingly without any disruption. Figure 13.6 shows natural examples of these relationships. In the intermediate case (synkinematic growth), the timing of growth and deformation coincide. The evidence for synkinematic growth is an external foliation that can be traced into a blast containing an internal foliation with a pattern different but connected to S_e . A classic example is a snowball garnet (Figure 12.13), where S_i spirals around the core of the garnet until it connects with S_e , which generally displays a simpler pattern.

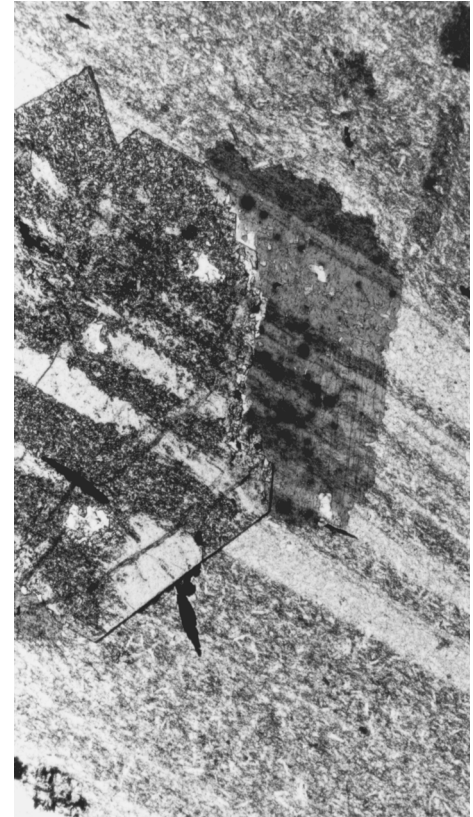
How do we preserve a spiral pattern in garnet and what can it tell us? Imagine a rock that becomes metamorphosed in an active shear zone. After a small porphyroblast nucleates, it rapidly grows by consumption and inclusion of other minerals (Figure 13.7). The shear zone foliation is incorporated into the blast as an inclusion trail. Because the mineral is affected by the shearing motion, like ball bearings between your hands (Section 12.4.1), continued mineral growth produces an internal foliation that appears to be rolled up, producing the characteristic snowball geometry. Now consider the alternative: the same pattern can be generated if the matrix rotates around a stationary, growing clast. Relative rotation of blast versus matrix is a matter of some debate and it has been suggested that blasts are located in non-deforming pods surrounded by bands that concentrate deformation. Most work, however, indicates that blasts rotate. Returning to our rocks, we are fortunate to find rotated garnets, so we conclude that metamorphism is synkinematic. Furthermore, the counterclockwise rotation sense supports the



(a)



(b)



(c)

FIGURE 13.6 Photomicrographs of [a] prekinematic, [b] synkinematic and [c] postkinematic growth of garnet [a and b] and staurolite [c]. Long dimension of view is ~1.5 mm.

reverse displacement in our mylonite zone that was also determined from other shear-sense indicators (see previous discussion).

In many instances we may not find evidence for synkinematic growth as compelling as that of snowball garnets. Nevertheless, it seems generally true that mineral reactions are triggered by deformation, because the stress gradients that exist during deformation promote material transport and grain growth (e.g., by fluid-assisted or “wet” diffusion; Chapter 9). Thus, mineral assemblages and mineral compositions may be metastable until deformation triggers the reactions that produce equilibrium assemblages for the ambient metamorphic conditions. While mineral growth dur-

ing deformation is common, it is not a rule. Environments of contact metamorphism, for example, are one exception.

13.4.1. Status Report II

From our latest observations we learn that previously determined P and T values represent the metamorphic conditions during deformation. In other words, deformation in the shear zone occurred under amphibolite-facies conditions. Much of the information necessary to solve our geologic mystery has been obtained, but we still don't know *when* these conditions of pressure and temperature prevailed. This has long been a diffi-

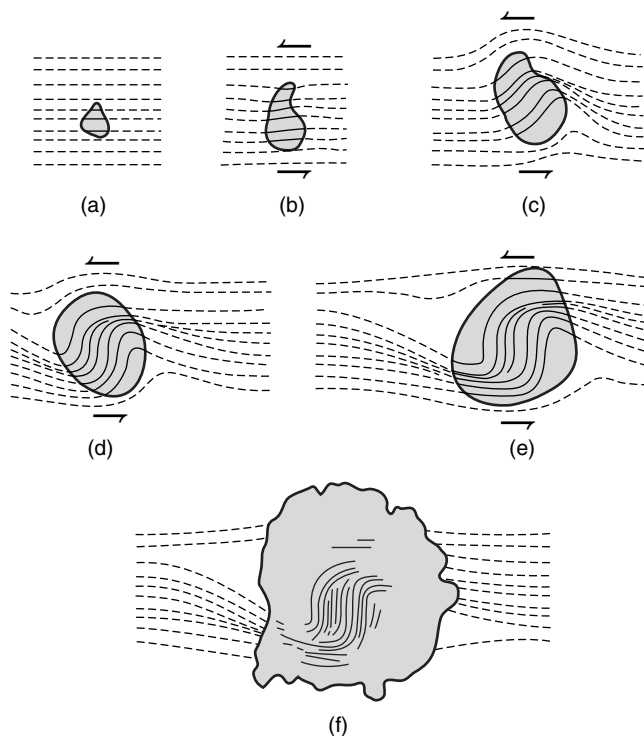


FIGURE 13.7 The progressive development of snowball textures in counterclockwise rotating, growing porphyroblast [a–f]. Compare the rotation with that in the garnet in Figure 13.6b.

cult question to answer, but huge progress in radiogenic isotope geochemistry comes to the rescue.

13.5 TIME

Minerals consist of a specific arrangement of atoms (crystal structure). Atoms, in turn, consist of protons and neutrons that make up the nucleus, which is surrounded by a cloud of electrons. The number of protons, the **atomic number** (symbol Z), defines an element; for example, Si contains 14 protons and its atomic number is therefore 14 (${}_{14}\text{Si}$). This atomic number specifies the order in the periodic table of the elements. The protons and neutrons combined define the mass of an atom, which is therefore called the **mass number** or **isotopic number** (symbol A). The mass number is the second value for an element that you find in the periodic table; for example Si has a mass of 28, which we place on the upper left of the element symbol: ${}^{28}_{14}\text{Si}$. In contrast to the atomic number, a single element can have several mass numbers; that is, different numbers of neutrons. For example the element rubidium has the isotopes ${}^{85}_{37}\text{Rb}$ and ${}^{87}_{37}\text{Rb}$. Some isotopes are unstable and they come apart spontaneously. Of the two Rb isotopes, ${}^{87}_{37}\text{Rb}$ is

unstable and decays to ${}^{87}_{38}\text{Sr}$. In this process we call rubidium the **parent isotope** and strontium the **daughter isotope**.⁴

The number of isotopes that decay per unit time is proportional to the number of parent isotopes; this proportionality factor is a constant for each unstable isotope and is called the **decay constant**, λ . Notice that isotope geologists use the same symbol that we previously defined as the quadratic elongation (Chapter 4); they are unrelated. Perhaps you are more familiar with the concept of **half-life** ($t_{1/2}$) of an isotope, which is the time required for half of a given number of parent isotopes to decay. For the transformation of Rb to Sr the decay constant is $1.4 \times 10^{-11}/\text{y}$, which means a half-life of $48.8 \times 10^9\text{y}$, based on the relationship

$$t_{1/2} = 0.693/\lambda \quad \text{Eq. 13.3}$$

Table 13.3 lists common radiogenic systems with their corresponding half-lives and decay constants.

The principle behind isotopic dating is simple. We measure the amount of parent (P) and daughter (D) in a mineral today. The sum of these equals the original amount of parent (P_0). The ratio D/P_0 is then proportional to the age of the mineral. A useful device to illustrate the fundamentals of geochronology is an hourglass. Starting with one side of the hourglass full (containing the “parent”) and the other side empty (representing the “daughter”), we only need to know the rate at which sand moves from one chamber to the other (the “decay constant”) and the amount of sand in the daughter chamber (or the amount of parent remaining) to determine how much time has passed. In mathematical terms

$$-dP/dt = \lambda P \quad \text{Eq. 13.4}$$

where dP/dt is the rate of change of the parent. This has a negative sign because the amount of the parent decreases with time. In practice, the process is a little more complex, as we will see next.

13.5.1 The Isochron Equation

The first complication arises at the time the radiogenic clock starts, because the rock already contains some daughter; in other words, some sand already exists in the daughter chamber before we start the timer. This amount of daughter is referred to as the **initial daughter**. When we measure the amount of daughter product in our

⁴There are no sons in this dating game.

TABLE 13.3		COMMONLY USED LONG-LIVED ISOTOPES IN GEOCHRONOLOGY			
Radioactive Parent (P)	Radiogenic Daughter (D)	Stable Reference (S)	Half-life, $t_{1/2}$ (10^9 y)	Decay constant, λ (y^{-1})	
^{40}K	^{40}Ar	^{36}Ar	1.25	0.58×10^{-10}	
^{87}Rb	^{87}Sr	^{86}Sr	48.8	1.42×10^{-11}	
^{147}Sm	^{143}Nd	^{144}Nd	106	6.54×10^{-12}	
^{232}Th	^{208}Pb	^{204}Pb	14.01	4.95×10^{-11}	
^{235}U	^{207}Pb	$^{204}\text{Pb}^1$	0.704	9.85×10^{-10}	
^{238}U	^{206}Pb	$^{204}\text{Pb}^1$	4.468	1.55×10^{-10}	

¹ ^{204}Pb is not stable, but has an extremely long half-life of $\sim 10^{17}$ years.
From Faure (1986).

specimen we are actually combining the amounts of daughter from decay of the parent and initial daughter. The latter amount needs to be subtracted for age determination. The solution to this problem involves using minerals of the same sample containing different isotopic ratios, which allows us to define an **isochron**. The details of this approach lie outside the scope of this chapter, but you will find them in every textbook on geochronology. We merely give you the **isochron equation** without more theory:

$$D/S = D_0/S + P/S (e^{\lambda t} - 1) \quad \text{Eq. 13.5}$$

where D is total amount of daughter present at time t (radiogenic and initial daughter), D_0 is common daughter, P is parent present at time t , S is a reference isotope (a stable, non-daughter isotope), λ is the decay constant, and t is time. You notice that this equation has the general form $y = a + bx$, which is the equation of a straight line. So, plotting the values of D/S and P/S for several minerals in a single rock defines a line (the isochron) whose slope represents the age of the sample; the slope is defined by $(e^{\lambda t} - 1)$ (Equation 13.5). An illustration is given in Figure 13.8 for the Rb-Sr system.

The situation is more complicated for the U/Pb system, because here we are dealing with two parents and two daughters (Table 13.3); however, this added complexity also results in great reliability for U/Pb ages. We simultaneously solve two isochron equations. If the ages are equal within error (typically within 2–3 m.y.), the age is called **concordant**; otherwise we have a **discordant** age (Figure 13.9). Discordant mineral ages are common and reflect loss of Pb after the mineral was formed, but they are not useless. Tech-

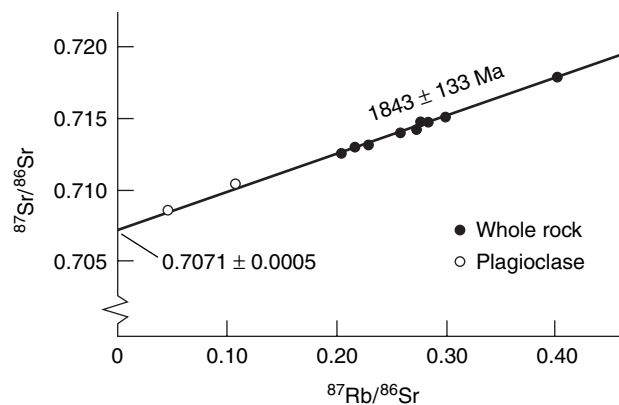


FIGURE 13.8 Rb-Sr isochron based on a combination of whole-rock analyses and plagioclase concentrates; each point represents an analysis. The different ratios lie on a straight line (the isochron) whose slope gives the age of the rocks.

niques to extract the original age of the mineral as well as the time of Pb loss have been developed. These properties and the high closure temperature for several minerals (see the following section) make U/Pb dating a very sensitive (standard error around 2 m.y.) and informative method that has become widely used in tectonics.

The $^{40}\text{Ar}/^{39}\text{Ar}$ method of dating is another geochronologic approach that we use in our study. The advantage of this method over traditional K-Ar determinations is that all measurements are carried out on the same sample (after neutron irradiation), allowing us to use a stepwise incremental heating technique, during which Ar is progressively released. In theory, the age obtained at each step (derived from the $^{40}\text{Ar}/^{39}\text{Ar}$ ratio) should be the same, but in practice this is generally not the case. Some Ar may have escaped

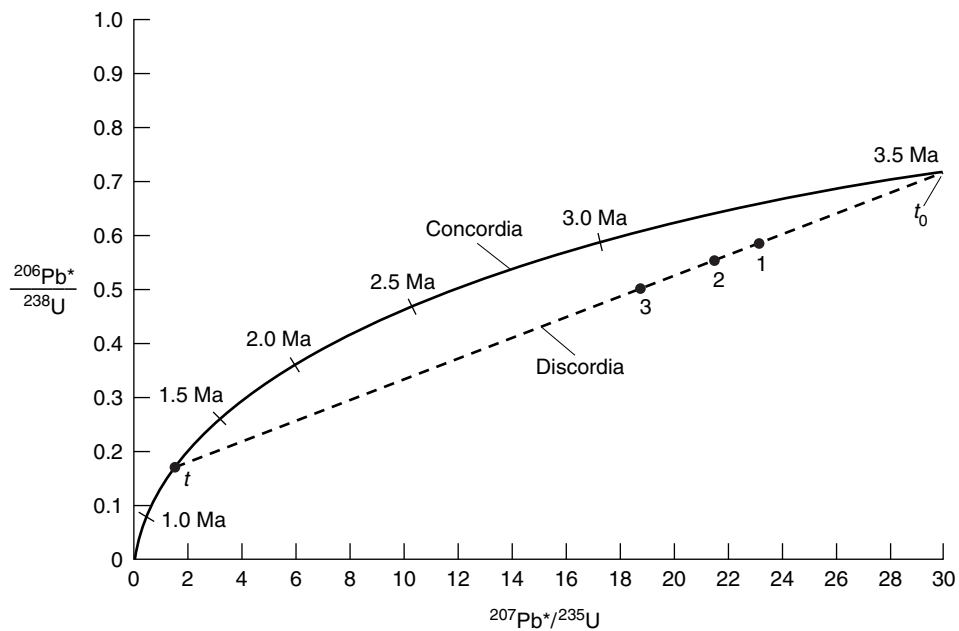


FIGURE 13.9 U-Pb concordia diagram showing three discordant zircon ages that reflect Pb loss at time $t = 1250$ Ma; the original zircon growth age is derived from the intersection between the line passing through the discordant zircon ages and concordia ($t_0 = 3500$ Ma). Modern U/Pb analysis uses portions or regions of individual grains to determine discordia. For example, the grain is progressive abraded to remove reset rims.

(called Ar-loss) or have been gained (called excess-Ar) in part of a mineral, which can be examined by stepwise release patterns (Figure 13.10); the details are outside the scope of this book. A reliable $^{40}\text{Ar}/^{39}\text{Ar}$ age for the mineral is aided by the recognition of a “plateau,” comprising several steps of equal age within some error limit. But before interpreting the radiometric data we need to understand the concept of closure temperature of a geochronometer.

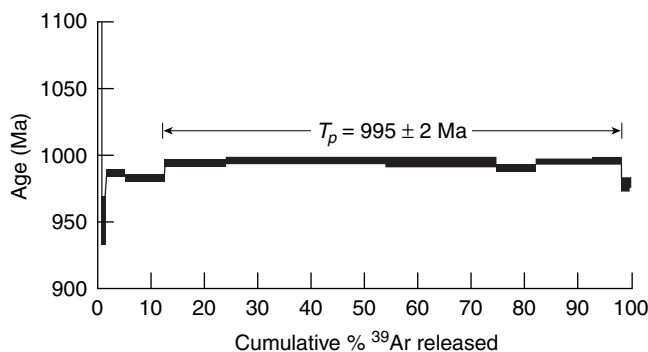


FIGURE 13.10 $^{40}\text{Ar}/^{39}\text{Ar}$ stepwise release spectrum of hornblende, with a plateau age, T_p , of 995 ± 2 Ma that is indistinguishable from the total gas age [also called the fusion age].

13.5.2 The Isotopic Closure Temperature

What does an isotopic age mean, or when does the radiogenic clock start? Previously you saw that the age of a mineral is a function of the ratio D/P . Now consider that the daughter chamber in our hourglass has a leaky bottom, so that the sand will not stay put until we close the chamber. Likewise, in nature, closure of the system for daughter product does not automatically coincide with the time of mineral growth nor does it occur at the same temperature for each isotopic system. This critical characteristic is addressed by the concept of the **closure temperature**, T_c . Below its closure temperature a mineral retains the amount of daughter produced; in other words, the radiogenic clock starts to tick upon reaching T_c . Above the closure temperature the daughter can escape. Table 13.4 lists closure temperatures for common minerals and their isotopic systems. Clearly, T_c differs for different minerals and isotopic systems. The closure temperature of a mineral is not a set value, but changes as a function of grain size (larger grains have higher T_c), cooling rate, and other parameters. The values listed in Table 13.4 are therefore based on common grain sizes, as well as on cooling rates that are typical of metamorphic rocks.

TABLE 13.4 **SELECTED CHRONOLOGIC SYSTEMS AND APPROXIMATE CLOSURE TEMPERATURES**

System-Mineral	T_c^1
U/Pb, zircon	>900°C
U/Pb, garnet	>800°C
U/Pb, monazite	725°C
U/Pb, titanite	600°C
U/Pb-rutile	400°C
$^{40}\text{Ar}/^{39}\text{Ar}$, hornblende	480°C
$^{40}\text{Ar}/^{39}\text{Ar}$, muscovite	350°C
$^{40}\text{Ar}/^{39}\text{Ar}$, biotite	300°C
$^{40}\text{Ar}/^{39}\text{Ar}$, alkali feldspar	350–200°C
Fission track-apatite	110°C
(U-Th)/He, apatite	~80°C

¹For a cooling rate of 1–10°C/m.y. and a common grain size; larger/smaller grain sizes have higher/lower T_c . After Mezger (1990) and other sources.

A high value of T_c implies that the radiogenic clock in a mineral is not easily reset by regional metamorphism, which explains, for example, the popularity of zircon U/Pb dating for formation ages of igneous rocks. Thus, dating porphyroblasts with a closure temperature that exceeds the metamorphic temperature (e.g., monazite and sphene in greenschist facies rocks) gives the *time of mineral growth*. Note that these minerals can grow at temperatures higher, equal to, or lower than T_c ! In general, analysis of minerals gives **growth ages** if the metamorphic temperature is less than T_c ; otherwise we obtain **cooling ages**. The difference in T_c for various minerals has advantages that are used in various ways to understand the history of a rock or region, as we'll see later.

13.5.3 Dating Deformation

Using our understanding of isotopic closure, growth, and cooling ages, we can finally turn to the question of when our rocks were deformed. Unfortunately, most “dateable” minerals are not involved in microstructures that reflect deformation. One solution is to bracket deformation by dating rocks that intrude the area; U/Pb ages on zircons from granites and peg-

matites are especially useful to this end. Deformed intrusive rocks give ages that predate the deformation, whereas undeformed intrusives are postkinematic. With some luck you constrain the deformation within tens of millions of years. In old rocks these constraints are often very loose, resulting in broad age brackets. Careful mapping may offer a second approach, involving intrusives that are restricted in their occurrence to deformation zones. This suggests that intrusion occurred due to deformation, so these synkinematic intrusives date the deformation. U/Pb zircon ages from pegmatites in Precambrian rocks are widely used for this purpose.

In our field area we find no dateable intrusions to bracket deformation, but we do have a range of minerals present that can be individually dated. Monazites and titanites in our mylonite show no evidence that they were derived elsewhere (i.e., eroded and transported). The crystals are euhedral and look “fresh,” and have distinctly different morphologies (color, size) from those in relatively undeformed samples elsewhere in the area. This indicates that they grew in our shear zone; they are synkinematic. Dating monazite and titanite using the U/Pb method gives us concordant ages of 1010 ± 2 Ma and 1008 ± 2 Ma, respectively. The closure temperature for monazite (725°C; Table 13.4) is well above peak metamorphic temperatures determined from thermometry (600°C), so this mineral grew below its closure temperature and, thus, dates the deformation. The titanite age is slightly younger, but the difference is not statistically significant (although it might reflect some resetting). Because the monazite represents a growth age, we conclude that the age of mylonitization is 1010 Ma.

Both approaches (dating of intrusives and dating of accessory phases) have drawbacks: (1) they do not date the mineral(s) involved in the mineral reactions on which we base the P and T conditions, and (2) they do not date minerals that are synkinematic based directly on microstructural relationships (as in Figure 13.5). In greenschist facies rocks this can be overcome by looking at mineral reactions involving hornblende, muscovite, and other phases that can be dated with the $^{40}\text{Ar}/^{39}\text{Ar}$ technique. In amphibolite facies rocks, however, this method only yields cooling ages, because T_c for these minerals (Table 13.4) is less than T_{peak} . As an option for high-grade rocks, garnets may be used for dating.⁵ This common mineral is involved in many geothermobarometric reactions (Table 13.1) and often

⁵There is some question as to whether U resides in the garnet or in inclusions; this ambiguity creates problems with high T_c inclusions.

allows determination of the relative timing of deformation and metamorphism (Figure 13.6). After considerable effort, U/Pb dating of synkinematic garnets in our samples produces an age of 1011 ± 2 Ma. This age is within the error of the monazite age and supports our previous determination for the age of deformation.

With our geochronologic work we have determined when deformation occurred, but we are also able to learn something about the subsequent history by dating other minerals. The range in T_c values for various systems gives an opportunity to constrain the cooling history of the area, an approach called **thermochronology**. If we date several minerals within a single rock we obtain the times at which the rock passes through the respective closure temperatures, provided that the minerals grew at or above their closure temperatures. In other words, we are able to calculate the temperature change per time unit (Figure 13.11). We apply the $^{40}\text{Ar}/^{39}\text{Ar}$ method to our gneiss sample, which yields ages for hornblende, muscovite, and biotite of 1000 Ma, 984 Ma, and 976 Ma, respectively. The **cooling rate** is the temperature difference divided by the age difference:

$$\text{cooling rate} = \delta T / \delta t \quad \text{Eq. 13.6}$$

In our sample, the cooling rate from the time of peak metamorphic temperature to the closure temperature for hornblende is:

$$(T_{\text{peak}} - T_{c,\text{hornblende}}) / (\text{age}_{\text{monazite}} - \text{age}_{\text{hornblende}}) = 120^\circ\text{C}/10 \text{ m.y.} = 12^\circ\text{C}/\text{m.y.}$$

Furthermore, if we calculate the cooling rate based on minerals with different ages, it appears that the cooling rate changes with time:

$$(T_{c,\text{hornblende}} - T_{c,\text{muscovite}}) / (\text{age}_{\text{hornblende}} - \text{age}_{\text{muscovite}}) = 130^\circ\text{C}/16 \text{ m.y.} = 8^\circ\text{C}/\text{m.y.}$$

$$(T_{c,\text{muscovite}} - T_{c,\text{biotite}}) / (\text{age}_{\text{muscovite}} - \text{age}_{\text{biotite}}) = 50^\circ\text{C}/8 \text{ m.y.} = 6^\circ\text{C}/\text{m.y.}$$

The decreasing cooling rate of our rocks places constraints on the uplift history of our area, as will be discussed after the third and final status report.

13.5.4 Status Report III

Our database has considerably expanded in size and scope since we hammered our samples in the field. Let's summarize the key information:

- Low-angle mylonite zone with reverse sense of displacement; based on field data and microfabrics.

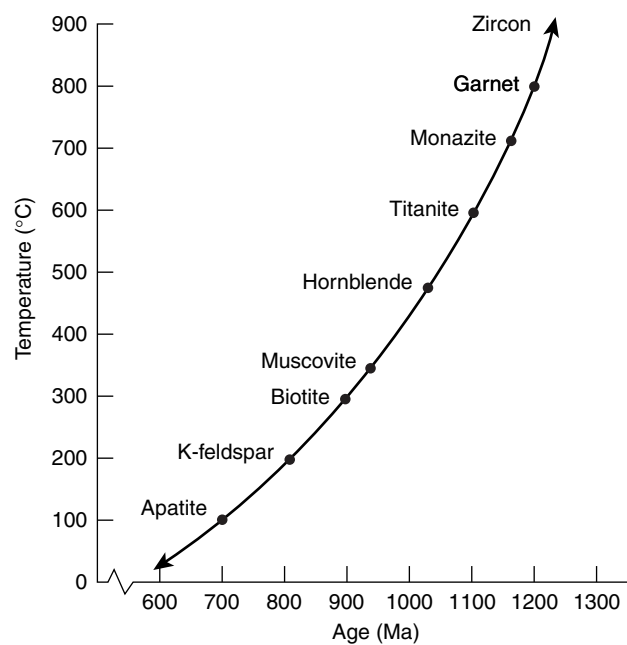


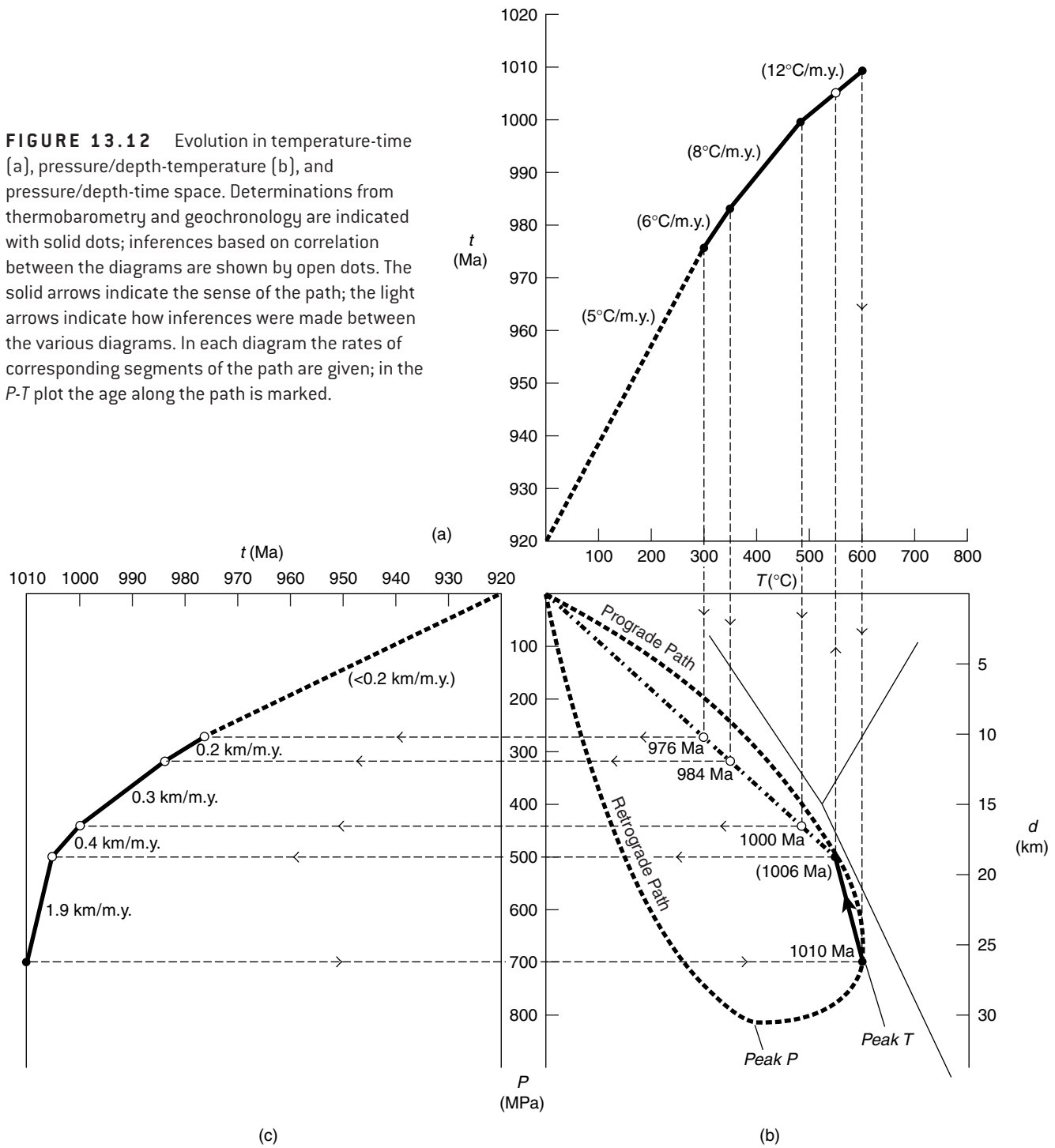
FIGURE 13.11 Schematic cooling history of a rock based on determining the ages of various minerals with different closure temperatures [see Table 13.4].

- Metamorphosed sediments; thus, originally deposited at the surface.
- Peak temperature of 600°C (middle amphibolite facies).
- Peak pressure of 700 MPa and burial depth of 26 km; thus, metamorphosed in the middle crust.
- 1010 Ma age of peak temperature and deformation (i.e., mid-Proterozoic orogenic activity) based on U/Pb ages of monazite and garnet.
- Retrograde metamorphic conditions of 500 MPa and 550°C based on garnet rim analyses.
- Cooling ages of 1000 Ma at 480°C , 984 Ma at 350°C , and 976 Ma at 300°C , based on hornblende, muscovite, and biotite $^{40}\text{Ar}/^{39}\text{Ar}$ dating, respectively.
- Cooling rate of $12^\circ\text{C}/\text{m.y.}$ during early retrogression that slows down to $6^\circ\text{C}/\text{m.y.}$

13.6 D-P-T-t PATHS

Status Report III provides quite a lot of information to digest, but we are now able to reconstruct a remarkably detailed history of our rocks, from deposition to burial and back to exhumation. This history is described by the pressure-temperature-time (P - T - t) path, which makes predictions about the deformation setting of the area. In Figure 13.12 the P , T , and t data that we collected (solid dots) and inferences based on them (open dots) are summarized in three related diagrams: a

FIGURE 13.12 Evolution in temperature-time (a), pressure/depth-temperature (b), and pressure/depth-time space. Determinations from thermobarometry and geochronology are indicated with solid dots; inferences based on correlation between the diagrams are shown by open dots. The solid arrows indicate the sense of the path; the light arrows indicate how inferences were made between the various diagrams. In each diagram the rates of corresponding segments of the path are given; in the *P-T* plot the age along the path is marked.



temperature-time diagram, a pressure (or depth)–temperature diagram, and a pressure (or depth)–time diagram. Each is explored separately in the following discussion.

13.6.1 Temperature-Time ($T-t$) History

Our careful geochronologic and thermochronologic work offers quite a few data points from which we may construct a reliable $T-t$ diagram. Each mineral age is plotted against the corresponding peak T or T_c , depending on whether it is a growth or cooling age, respectively. From this plot we see that the curve is not linear, but that it decreases in slope toward the surface temperature (for convenience we place the surface temperature at 0°C). Each segment of the curve has a different cooling rate that changes from 12°C/m.y. to 8°C/m.y. to 6°C/m.y. ; the youngest segment is unconstrained other than that it must intersect the T -axis at 0°C . We use a gradient of 5°C/m.y. , so that the rocks are at the surface around 920 Ma (heavy dashed line in Figure 13.12a).

13.6.2 Pressure-Temperature ($P-T$) History

In $P-T$ space we have determined two points from thermobarometry: 700 MPa and 600°C , and 500 MPa and 550°C . We also know from the occurrence of retrograde rims on garnet that the change in P and T trends toward the lower values, so we should have a counterclockwise sense for this part of the $P-T$ path. In addition, we know that the path should intersect the origin after 976 Ma (dashed line in Figure 13.12b), because the rocks are now at the surface. With the temporal information we can place ages at points where the $T-t$ curve intersects the $P-T$ curve. This exercise highlights an important characteristic of $P-T$ paths: there is no simple relationship between length of a $P-T$ path segment and length of time. A $P-T$ segment early in the retrograde history represents only a few m.y., whereas in the late history a segment of equal length represents tens of millions of years. The time at which we reach the $P-T$ point at 500 MPa and 550°C is predicted from the $T-t$ curve to be 1006 Ma. Note that the path from peak temperature to surface exposure, the **retrograde path**, is most likely smooth rather than kinked, as in Figure 13.12b (marked by the dashed line).

We have no direct information on the **prograde path**, before the rocks reached peak metamorphic conditions, other than that the path starts at the origin (when the rocks were deposited as sediments). We

simply connect the high-temperature end of our retrograde path with the origin (Figure 13.12b) to complete the $P-T$ path.

13.6.3 Pressure-Time ($P-t$) History

Only one point is constrained in $P-t$ space by barometric and chronologic work: 700 MPa at 1010 Ma. Nevertheless we are able to construct a $P-t$ path by combining the $T-t$ and $P-T$ curves (Figure 13.12c). The resulting path is a pattern of decreasing pressure change with time, which means a decreasing rate of removal of the overlying rock column with time (or decreased **exhumation rate**).⁶ For our purposes it is most informative to convert pressure to depth (1 km = 27 MPa); this shows that the exhumation rate changes by at least one order of magnitude, from approximately 2 km/m.y. to <0.2 km/m.y.

13.6.4 The Geothermal Gradient

The diagrams in Figure 13.12 highlight a second property of the crust's thermal structure in deformational settings: the geothermal gradient is not a constant. This gradient of temperature (T) change with depth (d) equals the ratio of cooling rate (Equation 13.6; Figure 13.12a) over exhumation rate (Figure 13.12b):

$$\text{geothermal gradient} = \delta T / \delta d \quad \text{Eq. 13.7}$$

Using Equation 13.7 for various time intervals constrained previously, we get

1010–1000 Ma	12°C/km
1000–984 Ma	26°C/km
984–976 Ma	30°C/km
976–(920) Ma	30°C/km

In other words, the value of the geothermal gradient changes with time, especially during the early retrograde history. Thus, no single geothermal gradient is representative for the entire orogenic history. Using the metamorphic P and T peak values only approximates the average geothermal gradient; therefore, the pattern is also called the **metamorphic field gradient**. In our area the average gradient is $600^\circ\text{C}/26$ km, or 23°C/km , which lies

⁶*Uplift* is sometimes used, but this describes displacement relative to a fixed coordinate system. Here we uplift the rock and remove its cover.

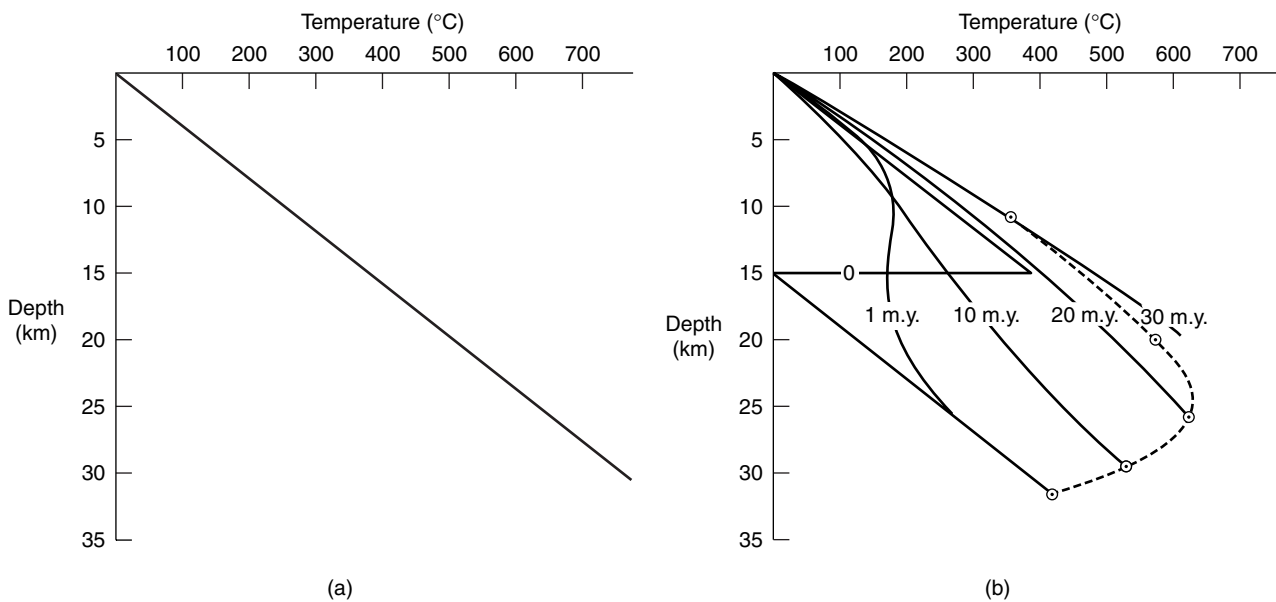


FIGURE 13.13 Thermal evolution after instantaneous doubling of a 15 km thick crustal section. A simplified geothermal gradient of $25^{\circ}\text{C}/\text{km}$ is assumed before thickening of the crust [a]. In [b] we show the geotherms at the time of instantaneous thrusting (0 m.y.), and after 1, 10, 20 and 30 m.y. After a few m.y. the irregularity in the thermal perturbation is largely removed, but the geothermal gradient remains depressed. After 10 m.y. the gradient is $<20^{\circ}\text{C}/\text{km}$; after 20 m.y. it is approximately back to the original value [$\sim 25^{\circ}\text{C}/\text{km}$], and after 30 m.y. the gradient is $30^{\circ}\text{C}/\text{km}$. Although these patterns are schematic, the shapes of the curves are based on thermal modeling.

in a reasonable range and agrees with values determined previously.

But why does the geothermal gradient change with time? Consider a slice of regular continental crust with an undisturbed geothermal gradient of $25^{\circ}\text{C}/\text{km}$ (Figure 13.13a). This gradient is not really linear, because heat-producing elements are preferentially concentrated in the upper crust, but for our purposes this simplification will do (in Chapter 14 we return to the thermal structure of Earth). At time t_0 , the top 15 km of the crust becomes doubled by thrusting. This results in a disturbed thermal gradient that steadily increases toward the thrust boundary, but at this boundary, sharply jumps back to the surface temperature, after which temperature again increases. This thermal pattern is called the **sawtooth model**. Note that the development of a sawtooth shape implies that deformation (here thrusting) is instantaneous relative to thermal equilibration. We can evaluate this.

The time over which a thermal perturbation decays by conduction is given by the “rule of thumb” equation for heat flow:

$$t = h^2/K \quad \text{Eq. 13.8}$$

where h is the distance over which thermal conduction occurs and K is the thermal diffusivity ($5 \times 10^{-7} \text{ m}^2/\text{s}$

for average crustal rock). Substituting $h = 15 \text{ km}$ gives an equilibration time on the order of 14 m.y. Although thrusting is not really instantaneous, it occurs at much faster rates than changes in thermal structure, permitting the simplification of geologically instantaneous deformation we just used. Equation 13.8 quantifies the change of a sawtooth thermal gradient with time, which we explore with a comforting analogy. Placing a hot blanket over your cold body creates a strong temperature gradient at the contact between blanket and skin. Pretty soon the heat of the blanket affects your body surface and the temperature difference becomes less. After a while there is little or no temperature contrast between blanket and skin, and you are comfortably warm. The actual thermal evolution is a bit more complex, because it also involves heat loss to the air and heat production by your body. But the analogy describes the situation in Nature pretty well. Before dozing off, we return to the cold reality of Figure 13.13b, where you see that after about 20 m.y. the original gradient is restored, and that after 30 m.y. it even exceeds the original value ($\sim 30^{\circ}\text{C}/\text{km}$). Thus, we conclude that deformation significantly affects the thermal structure of the crust for time periods of up to tens of millions of years. Note that adding contemporaneous erosion to our history further affects the thermal evolution.

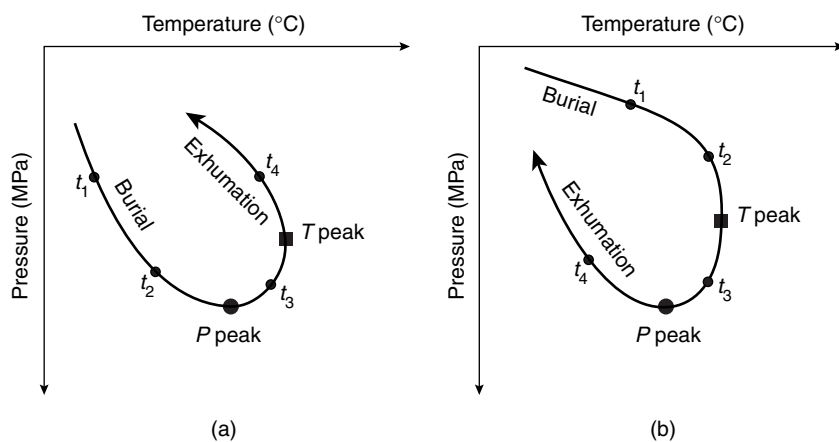


FIGURE 13.14 Counterclockwise (a) and clockwise (b) P - T - t paths may reflect characteristic deformation histories. Peak temperature [square] and peak pressure [circle] do not occur at the same time. Because metamorphic reactions proceed faster at peak temperatures, metamorphic pressures obtained from geothermobarometry are generally less than peak pressures. Note that the time steps [t_i] do not represent equal time increments.

13.6.5 The Deformational Setting

At the end of a chapter that seems dominated by metamorphic petrology and geochronology, we return to the “ D ” in D - P - T - t paths: deformation. The patterns in Figures 13.12 and 13.13 can be constructed and analyzed using numerical models involving input parameters describing heat production and heat transfer, and familiar parameters such as density, time, and depth. The theoretical approach, the details of which remain outside the scope of our discussion, can give critical insights into orogenic evolution. Observations on natural rocks, such as in our study, combined with modeling have produced characteristic relationships between P - T - t paths and the deformation history. For example, crustal thickening by thrusting results in rapid burial of rocks (deformation is relatively instantaneous; see previous discussion), a geothermal gradient that changes from a sawtooth shape to elevated values, and peak pressures that precede peak temperatures (Figure 13.14a). As a consequence of the latter, rocks record pressure at the time of peak temperature, which may differ from peak pressure. Our combined burial (prograde) and exhumation (retrograde) history describes a *counterclockwise path*⁷ (Figure 13.14a), which fits well with the analysis of our field observations and P - T - t data.

Paths from other tectonic environments have similarly characteristic geometries; for example, a clockwise path (Figure 13.14b) may reflect increasing heat from below due to extension and crustal thinning, or adding a heat source at the base of the crust (a process called **metamorphic underplating**). While numerical models do not substitute for observations, they can constrain part of the history that is not preserved in

natural rocks. Modeling, however, requires a critical attitude, because the input parameters may vary considerably and the equations are quite sensitive to uncertainties.

13.7 CLOSING REMARKS

Modern structural analysis integrates a variety of approaches. This essay offers only a glimpse of the possibilities that move structural geology into the full realm of orogenic evolution and tectonic processes of the deeper crust. Different disciplinary approaches have their strengths and weaknesses, but combined they provide internally consistent information to determine a more complete scenario. A crucial component in all this remains good field observations. There is no sense in analyzing a sample with highly sophisticated techniques and numerical models if the results are not representative for the area. Once we have met these requirements, an integrated approach, such as illustrated in this essay, will greatly expand our understanding of the tectonic history of a region and provide fundamental information on lithospheric processes. With these remarks we close the part of the book on ductile structures and move to the fundamentals of plate tectonics and lithospheric structure.

ADDITIONAL READING

Barker, A. J., 1990. *Introduction to metamorphic textures and microstructures*. Blackie: Glasgow.
 Bell, T. H., Johnson, S. E., Davis, B., Forde, A., Hayward, N., and Wilkins, C., 1992. Porphyroblast inclusion-tail orientation data: eppure non son girate! *Journal of Metamorphic Geology*, 10.

⁷Petrologists often plot pressure up, thereby creating a clockwise path; this generates terminology confusion with structural geologists plotting pressure/depth down.

- England, P. C., and Thompson, A. B., 1984. Pressure-temperature-time paths of regional metamorphism I. Heat transfer during the evolution of regions of thickened continental crust. *Journal of Petrology*, 25, 894–928.
- Essene, E. J., 1989. The current status of thermobarometry in metamorphic rocks. In Daly, J. S., Cliff, R. A., and Yardley, B. W. D., eds., *Evolution of metamorphic belts*. Geological Society Special Publication, 43, 1–44.
- Faure, G., 1986. *Principles of isotope geology* (2nd edition). J. Wiley & Sons; New York.
- Hodges, K. V., 1991. Pressure-temperature-time paths. *Annual Reviews of Earth and Planetary Sciences*, 19, 207–236.
- Mezger, K., 1990. Geochronology in granulites. In Vielzeuf, D., and Vidal, P., eds., *Granulites and crustal evolution*. Kluwer, pp. 451–470.
- Passchier, C. W., Meyers, J. S., and Kroner, A., 1990. *Field geology of high-grade gneiss terranes*. Springer Verlag.
- Passchier, C. W., Trouw, R. A. J., Zwart, H. J., and Vissers, R. L. M., 1992. Porphyroblast rotation: eppur si muove? *Journal of Metamorphic Geology*, 10, 283–294.
- Spear, F. S., and Peacock, S. M., 1989. Metamorphic pressure-temperature-time paths. *American Geophysical Union, Short Course in Geology*, 7.
- Spry, A., 1969. *Metamorphic textures*. Pergamon: Oxford.
- Vernon, R. H., 1976. *Metamorphic processes*. Murby: London.
- Villa, I. M., 1998. Isotopic closure. *Terra Nova*, 10, 42–47.
- Wood, B. J., and Fraser, D. G., 1977. *Elementary thermodynamics for geologists*. Oxford University Press.
- Zwart, H. J., 1962. On the determination of polymetamorphic mineral associations, and its application to the Bosost area (central Pyrenees). *Geologische Rundschau*, 52, 38–65.